



NIH Public Access

Author Manuscript

Biochemistry. Author manuscript; available in PMC 2014 June 11.

Published in final edited form as:
Biochemistry. 2013 June 11; 52(23): 4026–4036. doi:10.1021/bi400284j.

Discrete Interactions Between Bacteriophage T7 Primase-Helicase and DNA Polymerase Drive the Formation of a Priming Complex Containing Two Copies of DNA Polymerase[†]

Jamie R. Wallen^{#,||}, Jerzy Majka^{#,||,Δ}, and Tom Ellenberger^{#,*}

Department of Biochemistry and Molecular Biophysics, Washington University School of Medicine, St. Louis, MO 63110

Abstract

Replisomes are multi-protein complexes that coordinate the synthesis of leading and lagging DNA strands to increase replication efficiency and reduce DNA strand breaks caused by stalling of replication forks. The bacteriophage T7 replisome is an economical machine that requires only four proteins for processive, coupled synthesis of two DNA strands. Here we characterize a complex between T7 primase-helicase and DNA polymerase on DNA that was trapped during the initiation of Okazaki fragment synthesis from an RNA primer. This priming complex consists of two DNA polymerases and a primase-helicase hexamer that assemble on the DNA template in an RNA-dependent manner. The zinc binding domain of the primase-helicase is essential for trapping the RNA primer in complex with the polymerase, and a unique loop located on the thumb of the polymerase also stabilizes this primer extension complex. Whereas one of the polymerases engages the primase-helicase and RNA primer on the lagging strand of a model replication fork, the second polymerase in the complex is also functional and can bind a primed template DNA. These results indicate that the T7 primase-helicase specifically engages two copies of DNA polymerase, which would enable the coordination of leading and lagging strand synthesis at a replication fork. Assembly of the T7 replisome is driven by intimate interactions between the DNA polymerase and multiple subunits of the primase-helicase hexamer.

The core elements of eubacterial replisomes include multiple copies of DNA polymerase complexed to a helicase that drives replication fork progression (1). The replication complex is rounded out by a single-stranded DNA binding protein, a processivity factor, and a clamp loader that come on and off the DNA during replication. Replisomes are dynamic machines that can exchange proteins and change structure to accommodate the discontinuous synthesis of Okazaki fragments on the lagging strand of the replication fork (1). At a minimum, only two copies of DNA polymerase would suffice to simultaneously copy two antiparallel DNA strands, but it was recently discovered that some replisomes contain additional copies of DNA polymerase that may enhance replication efficiency. The best studied example is the

[†]This work was supported by a grant from the National Institutes of Health (GM055390) to TE.

[#]To whom correspondence should be addressed. Tel.: 314-362-2974, tome@biochem.wustl.edu.

^{||}Department of Biochemistry and Molecular Biophysics, Washington University School of Medicine, 660 South Euclid Avenue, St. Louis, MO 63110, USA

^ΔPresent address: Theranos Inc. 1601 S California Ave. Palo Alto, CA 94304

^{||}These authors contributed equally to this work.

Supporting Information

Supporting Information Available: Two figures are available. Figure S1 demonstrates the ability to isolate an RNA-dependent priming complex between gp4AZBD and gp5/Trx on ssDNA. Figure S2 is provided to show that Trx is not required for priming complex assembly. This material is available free of charge via the Internet at <http://pubs.acs.org>.

Escherichia coli replisome, where both *in vitro* and *in vivo* data provide strong support for three copies of DNA polymerase in an active replisome (2–5).

The *E. coli* replisome contains three copies of the clamp loader tau subunit that bind to three molecules of DNA polymerase (4). The gamma and tau subunits of the clamp loader are products of the dnaX gene, with gamma being a truncated protein as a result of a ribosomal frame shift (6). Both DNA Pol III and DnaB helicase interact with the C-terminus of the tau subunit, which is not present in gamma (7–9). Although it was originally thought that the *E. coli* clamp loader contains two copies of tau and one copy of gamma, single molecule experiments performed *in vivo* have demonstrated that the *E. coli* clamp loader actually contains three copies of tau, which can bind with a 1:1 stoichiometry to three molecules of DNA polymerase (4, 5). The proposed function of a third polymerase is to increase the processivity of the replisome and to aid in lagging strand DNA synthesis (3).

Bacteriophages T4 and T7 have long served as model systems to study the mechanisms of DNA replication due to their relative simplicity while recapitulating the essential activities of more complex eukaryotic replication systems (10–14). The bacteriophage T7 replisome is a model of simplicity with only four proteins required for efficient, coupled DNA replication *in vitro* (13). The gene 5 DNA polymerase (gp5) and its processivity factor, *E. coli* thioredoxin (Trx), form a 1:1 complex that functions in leading strand and lagging strand synthesis. The gene 4 primase-helicase (gp4) is a dual function enzyme catalyzing template-directed RNA primer synthesis with its N-terminal primase domain and unwinding the DNA template with its C-terminal helicase domain. Gene 2.5 single-stranded DNA (ssDNA) binding protein (gp2.5) coats the nascent ssDNA and binds to gp4 and gp5/Trx. The complete assembly of T7 replication proteins coordinately synthesizes both leading and lagging strands with a processivity of ~17 kilobases (15). Unlike the *E. coli* replisome, the T7 system does not utilize a clamp loader or a dedicated processivity factor that encircles DNA. Instead, the core replisomal protein gp4 encircles the DNA and directly interacts with the gp5/Trx polymerase to coordinate RNA primer synthesis, DNA unwinding, and DNA synthesis.

The dynamic structure of the T7 replisome is underscored by the alternative interactions between T7 replication proteins on and off DNA that involve different domains of gp4 and gp5/Trx. For example, an electrostatic interaction between the acidic C-terminal tail of gp4 and two different basic patches on gp5/Trx occurs in the absence of DNA (16). The acidic tail of gp4 binds to one of the basic patches, the front basic patch located in the DNA binding groove of gp5, in order to help load the polymerase on DNA (16). The interaction with the second basic patch, located in the Trx binding domain of gp5, functions both to keep a polymerase that has disengaged from DNA tethered to a moving replisome and also allows a polymerase from solution to exchange with a polymerase already associated with a moving replisome (15, 17). The interaction with the Trx binding domain increases the processivity of the T7 replisome (15). Once gp5/Trx engages DNA, the C-terminal tail of gp4 is no longer essential for gp5/Trx binding but is still predicted to bind the front basic patch of gp5 (18).

On the lagging strand of the T7 replication fork, the N-terminal primase domain of gp4 initiates the synthesis of Okazaki fragments by polymerizing oligoribonucleotides to prime DNA synthesis by the gp5/Trx polymerase. The tetraribonucleotides synthesized by the gp4 primase are not readily extended by gp5/Trx alone, requiring gp4 to stimulate primer utilization by gp5/Trx through an intermolecular handoff (19, 20). The N-terminal zinc binding domain (ZBD) of the gp4 primase-helicase is essential for primer synthesis and phage growth (21, 22). High concentrations of the ZBD alone can stimulate primer utilization by gp5/Trx (23), although it is not absolutely required to prime DNA synthesis

from a ribooligonucleotide *in vitro* (24). The priming complex that hands off the RNA primer from gp4 to gp5/Trx can be trapped in a stable complex on DNA by incorporating a chain terminating 2',3'-dideoxy nucleotide into the elongating RNA primer (19, 20, 25). The correct incoming nucleotide matching the DNA template is additionally required to lock gp5/Trx on to the RNA:DNA substrate. These conditions trap the gp5/Trx polymerase on a template DNA annealed to a longer primer strand (26), whereas the gp4 protein is additionally required to stabilize the primer extension complex with a tetraribonucleotide primer (19, 20, 23). The T7 priming complex provides a snapshot of a replication intermediate that is generally informative about the protein composition and shape of the T7 replisome as well as the mechanisms for coupling their enzymatic activities during replication.

The *E. coli* replisome incorporates three copies of DNA polymerase through their interactions with the tau subunit of the clamp loader (3, 4). In the T7 replisome, the gp4 primase-helicase loads as a hexamer on ssDNA (27) and directly contacts the gp5/Trx polymerase, raising the possibility that up to six copies of the T7 DNA polymerase could associate with the T7 replisome. However, the constraints of DNA binding and protein-protein interactions within the replisome are likely to further limit the number of subunits and their orientations. We examined the subunit composition of the T7 priming complex bound to a ssDNA or a model replication fork, and find that two copies of the gp5/Trx polymerase associate with a gp4 hexamer in the RNA-dependent priming complex. These data support a model in which each copy of the gp5/Trx polymerase is associated with multiple subunits of the gp4 hexamer, excluding additional copies of DNA polymerase from the complex. This subunit composition suggests that the T7 replisome is assembled through stable protein-protein interactions that in turn dictate interactions with the DNA substrate.

Materials and Methods

Oligonucleotides and Proteins

All deoxynucleotides were synthesized on a 1 μmol scale using an Applied Biosystems 394 DNA/RNA synthesizer, gel purified, and desalted using SepPak cartridges (Waters Inc.). RNA substrates were purchased from Dharmacacon. To generate primed templates and fork-shaped substrates, equal concentrations of complimentary oligonucleotides were mixed in 10mM MES pH 6.5, 40mM NaCl, heated to 95°C, then allowed to slowly cool to room temperature in a water bath. All DNA and RNA substrates used in this study are summarized in Table I.

Full-length wild-type gp4, gp4ΔZBD, and gp4CΔ17 proteins were expressed in BL21(DE3)pLysS cells and purified to homogeneity using polyethylene glycol 4000 precipitation followed by phosphocellulose, monoQ, and Superdex 200 chromatography. Gp4E343Q was expressed in HMS174(DE3) cells and purified using the same protocol as for wild-type gp4. The gp4E343QCAΔ17 mutant was generated by site-directed mutagenesis using the gp4CΔ17 plasmid as the template and was expressed and purified as described for wild-type gp4. T7 produces both full-length gp4 and the gp4ΔZBD protein during infection, with gp4ΔZBD production resulting from an internal start codon at position 64 (21). Our studies utilized gp4 expression constructs in which the methionine 64 codon was mutated to encode glycine in order to prevent expression of the N-terminally truncated gp4ΔZBD protein (21, 28). The exonuclease deficient gp5_{5A7A} polymerase (29) was used for all experiments, and purified as described previously (26). The gp5_{5A7A} Δ401–404 mutant was generated by PCR and was subcloned between the NdeI and XhoI sites of pET21b. The gp5_{5A7A} Δ401–404 mutant was expressed and purified using the same protocol as for gp5_{5A7A}.

Surface Plasmon Resonance

Surface plasmon resonance experiments were performed using a BIACore X instrument in buffer containing 25 mM Tris pH 7.5, 200 mM NaCl, 10 mM MgCl₂, 5 mM DTT, 0.1% NP-40, 100 µg/mL BSA, and indicated concentrations of dTTP. 0.2 mg/mL streptavidin (final volume of 100 µL in 10 mM sodium acetate pH 4.5) was coupled to a CM5 chip derivatized with N-hydroxysuccinimide and N-ethyl-N-(dimethylaminopropyl)carbodiimide, then 150–200 resonance units of biotinylated DNA containing a primase recognition sequence was attached to the chip at a flow rate of 5 µL/min. Priming complex formation was monitored at 25°C by injecting 70 µL at a flow rate of 20 µL/min. Priming complexes containing 1 µM gp4 hexamer, 1 µM gp5/Trx, 0.2 µM terminated RNA primer and 1 mM of the correct incoming nucleotide (dTTP) were injected on the chip at flow rate of 6 µL/min.

Isolation of the priming complex using streptavidin magnetic beads

To determine protein stoichiometry, the priming complex was formed on a 3'-biotinylated 19-mer ssDNA template attached to Dynabeads M-280 streptavidin magnetic beads (250 pmols of DNA per 20 µL of beads) in buffer consisting of 25 mM Tris pH 7.5, 200 mM NaCl, 10 mM MgCl₂, 5 mM DTT, 0.1% NP-40, and 100 µg/mL lysozyme. The binding reaction (100 µL) was carried out at 25°C for 30 min and contained 0.5 µM gp4 hexamer, 0.5 or 3 µM gp5/Trx, 0.5 µM terminated primer, 2 mM dTTP, and 25 µM poly-dT 25-mer to serve as a competitor. The beads were washed 4 times with 500 µL of buffer containing 1 mM dTTP and resuspended in 15 µL of SDS-PAGE loading buffer. Protein components of the complex were analyzed by 10% SDS-PAGE electrophoresis followed by Sypro Ruby staining and quantified by fluorescence imaging. The band intensities were converted to protein concentrations using a calibration gel (Figure 2B).

To measure the ability of different gp4 proteins to form the priming complex, 100 µL reactions were incubated at 25°C for 10 minutes in 25 mM Tris pH 7.5, 200 mM NaCl, 10 mM MgCl₂, 5 mM DTT, 0.1% NP-40, 100 µg/mL lysozyme, and 25 µM poly-dT trap on 3'-biotinylated 19-mer ssDNA. Both Thermo MagnaBind and Spherotech streptavidin magnetic beads were used in these experiments. Beads were washed 4 times with 90 µL of buffer containing 2 mM dTTP and 5 µM poly-dT trap and resuspended in 10 µL of SDS-PAGE loading buffer. Protein components of the complex were analyzed by 10% SDS-PAGE electrophoresis followed by Sypro Ruby staining. For figure 3, 2 µM gp5/Trx was mixed with 1 µM hexamer of either wild-type full-length gp4, gp4E343Q, or gp4CΔ17 along with 0.5 µM terminated primer and 2 mM dTTP. For figure 7, 2 µM gp5/Trx was mixed with 1 µM wild-type full-length gp4 hexamer, 2.5 µM terminated primer, and 2 mM dTTP on either a 31-mer 3'-biotinylated ssDNA substrate or a fork shaped substrate. The fork substrate contained a 20 base pair complimentary region with a 31-mer ssDNA 5'-tail, a 33-mer 3'-biotinylated tail, and a 21-mer primer annealed to the 3'-tail.

Primer extension assays

Primer extension reactions (20 µL) were carried out at 25°C in 25 mM Tris pH 7.5, 200 mM potassium glutamate, 10 mM MgCl₂, 5 mM DTT, 0.1% NP-40, and 100 µg/mL BSA and contained 20 µM template DNA, 0.5 µM gp4 hexamer, 2.5 µM gp5/Trx, 2 mM dTTP, 50 µM 5'-labeled ACCC primer, and 0.5 mM dNTPs. Reactions were stopped after 3 and 30 minutes by quenching 5 µL aliquots with an equal volume of formamide containing 20 mM EDTA. Samples were analyzed on 25% acrylamide 4M urea sequencing gels followed by phospho-imaging.

DNA extension reactions within the isolated priming complex contained ~0.1 µM of the isolated complex, 2 mM dTTP, and 50 nM duplex DNA prepared by annealing a 17-mer

primer (labeled at the 5' end with [γ -³²P]-ATP and T4 polynucleotide kinase) with a 30-mer template.

Where indicated, the reactions additionally contained 0.5 mM dCTP, 0.2 mM ddATP, and 10 mM dGTP. After a 15 minute incubation half of the reaction (10 μ L) was stopped by quenching with formamide containing 20 mM EDTA. The priming complex from the remaining reaction was isolated using magnetic beads and washed three times with buffer containing 2 mM dTTP and 5 mM dGTP, then resuspended in formamide containing 20 mM EDTA. Samples were analyzed on 25% acrylamide 4M urea sequencing gels followed by phospho-imaging.

Analytical ultracentrifugation

All centrifugation experiments were performed with an Optima XL-A analytical ultracentrifuge using an An60Ti rotor (Beckman Coulter). Experiments were performed at 22°C in 25 mM Tris pH 7.5, 200 mM NaCl, 10 mM MgCl₂, 2 mM DTT, 5 mM dTTP, and 20% glycerol. Sedimentation velocity measurements were performed at 35000 RPM using an Epon charcoal-filled double-sector centerpiece. 3 μ M gp4E343QC Δ 17 hexamer was mixed with 6 μ M fluorescein-labeled 20-mer ssDNA, 7.2 μ M terminated RNA, and the indicated concentrations of gp5/Trx, and samples were scanned every 8 minutes at 495 nm at a spacing of 0.03 cm. The ssDNA, terminated RNA primer, and incoming nucleotide (dTTP) are all present in excess relative to the proteins in order to saturate the complex. Sedimentation velocity profiles were analyzed using Sedfit (Peter Schuck (Dynamics of Macromolecular Assembly Laboratory of Cellular Imaging and Macromolecular Biophysics, National Institutes of Health, Bethesda MD)) (30) and the sedimentation coefficients were corrected for buffer and temperature using SEDNTERP (Thomas Laue (University of New Hampshire, Durham, NH)). Partial specific volumes for gp4E343QC Δ 17 and for the gp4E343QC Δ 17:gp5/Trx complex were calculated from amino acid composition to be 0.7304 mL/g and 0.7356 mL/g, respectively. The buffer density was calculated to be 1.0652 g/cm³.

Sedimentation equilibrium experiments were performed using an Epon charcoal-filled six-sector centerpiece at rotor speeds of 5000, 7000, and 9000 RPM. 3 μ M gp4E343QC Δ 17 hexamer was mixed with 2 μ M fluorescein-labeled 20-mer ssDNA, 2.4 μ M terminated RNA, and the indicated concentrations of gp5/Trx. Samples were scanned at 495 nm every 4 hours at 0.01 cm spacing, with each scan taken as an average of three scans. Equilibrium scans were analyzed using Sedfit/Sedphat (31). All centrifugation figures were prepared using the program GUSSI (Chad Brautigam (Department of Biophysics, The University of Texas Southwestern Medical Center at Dallas, Dallas, TX)).

DNA unwinding assays

DNA unwinding assays were performed at room temperature in 25 mM Tris pH 7.5, 40 mM NaCl, 10 mM MgCl₂, 10 mM DTT, 100 μ g/mL BSA, and 10% glycerol. DNA fork substrates for unwinding were generated by annealing oligonucleotides with 20 base pair complimentary sequences to generate a 31-mer 5'-tail and a 20-mer 3' poly dT tail labeled with fluorescein. An 18-mer poly dA annealed to the 3'-tail mimicked a leading strand synthesis product. 2 μ M gp4 hexamer and 4 μ M gp5/Trx were incubated with 100 nM labeled DNA substrate, 1 μ M RNA primer, and 10 mM dTTP for 30 minutes in Mg⁺⁺-free buffer containing 1 mM EDTA. Reactions were initiated by addition of an equal volume of 2X buffer containing 10 mM MgCl₂ and 10 μ M ssDNA trap; the trap in these reactions serves to both sequester protein not bound to the fork and to prevent re-annealing of the fork substrates. Reactions were quenched at 2, 5, and 30 minutes by mixing 10 μ L of the reaction with an equal volume of 100 mM EDTA, 0.4% SDS, and 20% glycerol. Reactions were

analyzed by running 8% native gels at 100 volts for 1 hour in 1X TBE buffer at room temperature, and DNA products were quantified by fluorescence imaging.

Results

Formation of a stable, functional T7 priming complex

Previous work demonstrated that priming complexes consisting of gp5/Trx together with the ZBD of gp4, the N-terminal primase domain of gp4, or a monomeric form of gp4 (19, 20, 23) could be trapped on a ssDNA containing the T7 primase recognition sequence (PRS) (32) in the presence of a dideoxy-terminated RNA primer and the correct incoming deoxynucleotide to lock gp5/Trx on the DNA. All of these gp4 constructs include the N-terminal ZBD of gp4, which is critical for complex assembly and for efficient RNA primer utilization by gp5/Trx (19). Using surface plasmon resonance we find that a stable priming complex assembles between gp5/Trx and full-length gp4 (Figure 1A). A stable complex forms on ssDNA only when gp4, gp5/Trx, a terminated RNA primer, and an incoming nucleotide are present. When any of these components are omitted, or if the correct incoming nucleotide (dTTP) is substituted with dCTP, the priming complex fails to assemble (Figure 1A). The incoming dTTP nucleotide serves two important roles in priming complex assembly, binding in the active site of gp5/Trx and stabilizing the gp4 hexamer on ssDNA (27). Although gp4 forms both hexamers and heptamers in vitro (33), only the gp4 hexamers are capable of binding DNA (34) and therefore likely to participate in the T7 priming complex. To minimize hydrolysis of dTTP we used a mutant gp4 (gp4E343Q) with a glutamine substituted for the glutamic acid residue serving as a general base for nucleotide hydrolysis in the helicase active site. The gp4E343Q mutant binds tightly to ssDNA but has no observable dTTP hydrolysis activity in the presence of a ssDNA substrate (35). Increasing the concentration of dTTP in the reaction buffer increases the stability of the priming complex and slows its dissociation from ssDNA (Figure 1A).

To confirm that the complex of gp5/Trx and full-length gp4 formed under these conditions can initiate DNA synthesis, we measured primer extension activity on a ssDNA template containing a PRS (Figure 1B). Whereas gp5/Trx alone does not efficiently extend an RNA primer complementary to the PRS, the combination of gp5/Trx with either wt gp4 or gp4E343Q effectively incorporates the primer into a DNA product (Figure 1B). Gp4 lacking the ZBD (gp4 Δ ZBD) has very little activity in the priming complex with gp5/Trx (Figure 1B) although these proteins can bind to the ssDNA (Supplementary Figure S1 and (25)). These results show that full-length gp4 and gp5/Trx form a functional priming complex that requires the ZBD of gp4 for priming complex assembly. By incorporating a 2',3'-dideoxynucleotide chain terminator early in the primer extension reaction the elongating polymerase is trapped on DNA, stabilizing the priming complex (19) and enabling analysis of its subunit makeup and structure.

Two copies of gp5/Trx assemble in the stalled T7 priming complex

The combination of a ssDNA oligonucleotide with a PRS and a complementary RNA primer provides a substrate for binding of the gp4 hexamer and one copy of gp5/Trx. Additional copies of the polymerase could be incorporated into the priming complex through protein-protein interactions. To investigate the protein stoichiometry on ssDNA we purified the T7 priming complex consisting of gp4, gp5/Trx, the correct incoming nucleotide (dTTP), and a terminated RNA primer on a biotinylated ssDNA substrate containing a PRS using streptavidin beads then analyzed the ratios of gp4 and gp5/Trx by SDS-PAGE and protein staining intensity. Figure 2 demonstrates that a priming complex can be purified on DNA only when gp4, gp5/Trx, dTTP, and a terminated RNA primer are all present. A quantitative analysis of the gel staining intensities calibrated with purified protein standards (Figure 2B)

reveals that two copies of gp5/Trx co-purify with a gp4 hexamer. Trx is not required for priming complex assembly, as gp5 lacking Trx also co-purifies with gp4 in an RNA-dependent manner (Supplemental Figure S2). This indicates that the protein interactions essential for priming complex formation occur between gp4 and gp5 and do not involve Trx. The T7 priming complex consists of a fixed 2:1 ratio of gp5/Trx and gp4 hexamer irrespective of the addition of limiting or excess gp5/Trx (Figure 2, lanes 4 and 6, respectively). The results demonstrate that at both limiting and saturating polymerase concentrations two copies of gp5/Trx co-purify with a gp4 hexamer in a priming complex that incorporates a lagging strand template for RNA-primed DNA synthesis. Although the DNA template in the priming complex has only one binding site for gp5/Trx, a second copy of gp5/Trx is stably incorporated into the replisome and could function in leading strand replication.

The gp4 helicase translocates on ssDNA using dTTP as the energy source to power DNA unwinding (36). Helicase activity could cause the priming complex to dissociate as gp4 translocates away from the PRS while depleting the dTTP pool required to trap gp5/Trx on DNA in the priming complexes studied here. We compared priming complexes formed with wild-type gp4 to the gp4E343Q mutant (Figure 3) and saw no difference in the efficiency of complex assembly based on the amounts of wild-type gp4 and gp4E343Q proteins that were pulled down. Additionally, there is no difference in the ratios of gp5/Trx:gp4 hexamer purified. This result indicates that wild-type gp4 is immobilized in the priming complex and unable to translocate on ssDNA. The results of DNA unwinding assays discussed below further support this conclusion.

We also examined the possible contribution of the C-terminal tail of gp4 to binding gp5/Trx in the priming complex with the mindset that one of the two polymerase molecules may interact with the acidic tail of gp4 via the previously described electrostatic binding mode (16). However, the C-terminal tail of gp4 is not required to stabilize the priming complex on ssDNA, in agreement with a recent report (25). Two copies of gp5/Trx co-purify with a mutant gp4 lacking the C-terminal tail (gp4C Δ 17; Figure 3).

Analysis of the protein stoichiometry in the T7 priming complex by analytical ultracentrifugation

To accurately assess the protein stoichiometry of the T7 priming complex, the native complex formed on ssDNA was analyzed by analytical ultracentrifugation (Figure 4). The high concentrations of nucleotide required to stabilize the priming complex (20, 25) interfered with monitoring protein absorbance at 280 nm, so a fluorescein-labeled 20-mer ssDNA in the complex was instead monitored at 495 nm. For these studies, we used a gp4 variant (gp4E343QC Δ 17) lacking the C-terminal tail to increase protein solubility, and with a helicase active site mutation that minimizes nucleotide hydrolysis. Neither the E343Q mutation nor the deletion of the C-terminal residues alters the assembly of the priming complex (Figure 3). Gp5/Trx was titrated against a fixed concentration of gp4 hexamer in the presence of fluorescein-labeled ssDNA, a terminated RNA primer, and dTTP, and the resulting complexes were analyzed by sedimentation velocity. Figure 4A shows representative velocity scans for a 1:1 ratio of gp5/Trx to gp4 hexamer in complexes with and without a terminated RNA primer. Addition of the RNA primer causes formation of a larger species bound to the DNA, indicative of priming complex formation. A smaller species attributed to the excess free ssDNA is also present in both samples.

In buffer containing low to moderate salt concentration, the gp4 hexamer binds to ssDNA in a sequence-independent manner (34, 37, 38). This nonspecific complex of gp4 on ssDNA sediments as a symmetrical peak with a sedimentation coefficient of 12.3 S (Figure 4B). A titration of gp5/Trx in the presence of an RNA primer and dTTP shifts the sedimentation

coefficient to higher values, saturating at a 2:1 molar ratio of gp5/Trx:gp4 hexamer with a sedimentation coefficient of 16 S (Figure 4B). Omission of the terminated RNA primer results in a sedimentation coefficient (12.5 S) that is similar to gp4 alone, indicating no priming complex forms in the absence of RNA. At sub-saturating concentrations of gp5/Trx the c(s) traces show broad peaks, indicative of multiple species in solution. This distribution sharpens with increasing concentrations of gp5/Trx that saturate the priming complex (compare the 0.5:1 and 2:1 input ratios in Figure 4B). A 2:1 complex of the gp5/Trx and gp4 hexamer is purified on streptavidin beads under conditions of limiting or excess polymerase concentration (Figure 2), which suggests that the multiple species observed in the centrifugation experiment represent a mixture of free gp4 on ssDNA and a 2:1 complex of gp5/Trx:gp4 hexamer. Finally, all of the c(s) distribution profiles show a minor species (less than 10 percent of the total distribution) representing higher order aggregates of the proteins (Figure 4B).

The buoyant mass of the priming complex was determined by sedimentation equilibrium centrifugation at 2:1, 3:1, and 6:1 input ratios of gp5/Trx:gp4 hexamer (Figure 5). A priming complex consisting of a gp4 hexamer, two molecules of gp5/Trx, ssDNA, and a terminated RNA primer has a predicted mass of 554,259 Da, while a priming complex with just one gp5/Trx would be expected to have a mass of 462,994 Da. Equilibrium scans of the labeled DNA at 5,000, 7,000, and 9,000 RPM are similar for the three different input ratios of proteins. The masses calculated from these DNA complexes are in good agreement with one another and range from 517,524 Da to 528,294 Da, which is consistent with a composition of two copies of gp5/Trx and a gp4 hexamer in the priming complex. Taken together, the velocity and equilibrium analytical ultracentrifugation results confirm that two molecules of gp5/Trx are stably associated with gp4 in the T7 priming complex.

The second DNA polymerase in the T7 priming complex can bind a primed template DNA

To address the functionality of the second gp5/Trx in the priming complex, we investigated the ability of a primed template DNA to co-purify with the T7 priming complex captured on an immobilized ssDNA containing the PRS (Figure 6). The priming complex was assembled in the presence of a terminated RNA primer and dTTP then purified on a biotinylated ssDNA substrate containing a PRS. After pulling down the priming complex, a radio-labeled DNA primer-template pair was added along with ddATP, dTTP, dCTP, and dGTP. If the second molecule of DNA polymerase in the priming complex can function in templated DNA synthesis then the radiolabeled primer-template should be trapped by the ddATP chain terminator and added dNTPs (with dGTP serving as the correct incoming nucleotide) and readily pulled down with the priming complex. Following incubation with the radiolabeled DNA and nucleotides, the priming complex was pelleted a second time with the streptavidin beads and analyzed using a sequencing gel. Figure 6 shows that the DNA primer-template co-purified with the priming complex only if DNA synthesis was terminated by ddATP (lane 9); no DNA was purified in the presence of dTTP only (lane 8) or in the presence of only dNTPs (lane 10). This demonstrates that the second copy of gp5/Trx in the complex is functional in DNA synthesis while the other DNA polymerase molecule remains bound to the RNA primer and the ssDNA immobilized on streptavidin beads (compare lanes 9 and 15). These binding activities demonstrate the presence of two functional copies of gp5/Trx in the priming complex, which could be representative of the leading and lagging strand polymerases at a replication fork.

The stalled priming complex locks gp4 on DNA and prevents helicase activity

During DNA replication, the hexameric gp4 helicase encircles the lagging strand of the replication fork to catalyze DNA unwinding and fork progression in a reaction requiring both magnesium and nucleotide (27, 39). To confirm that gp4 is loading productively onto

DNA under our experimental conditions we investigated priming complex formation on a fork-shaped DNA substrate resembling a replication fork (Figure 7). As with the ssDNA substrate, the priming complex can be stabilized on an artificial replication fork by addition of a terminated RNA primer with the correct incoming dNTP specified by the lagging strand template (Figure 7A). A non-terminated ACCC primer allows the incoming nucleotide to be incorporated by the polymerase then released, failing to stabilize the proteins on the DNA template (Figure 7A). Only in the presence of the terminated RNA primer can both gp4 and gp5/Trx be purified on a model replication fork, in agreement with the results on ssDNA. The priming complex also requires magnesium in the buffer to facilitate nucleotide binding in the active site of gp5/Trx (40), as no complex is purified in the presence of a terminated RNA primer when magnesium is omitted from the buffer (data not shown). The similar staining intensities of proteins bound to a fork-shaped DNA and ssDNA suggest that two molecules of gp5/Trx are bound in the priming complex on a forked substrate as shown above for the complex on ssDNA (Figures 2–5).

To confirm functional loading of gp4 on a forked DNA, we monitored DNA unwinding activity in the presence of gp5/Trx and both non-terminated and terminated RNA primers (Figure 7B). The complexes were pre-assembled on the fork in the absence of magnesium (27) and unwinding was initiated by addition of magnesium and a DNA trap to prevent rebinding of dissociated proteins and re-annealing of the unwound DNA strands. The gp4 helicase unwinds the fork substrate in the presence of a non-terminated ACCC primer, demonstrating that gp4 is in fact properly loaded and can translocate on the 5' tail of the fork to catalyze DNA unwinding (Figure 7B). In contrast, by locking the proteins on DNA in a chain terminated priming complex, fork progression and unwinding are effectively blocked (Figure 7B), confirming that the priming complex is properly oriented on the fork substrate, and remarkably, that the complex is stable enough to tether gp4 in place and prevent DNA unwinding. Gp4 rapidly unwinds the forked DNA in the presence of the terminated RNA primer if gp5/Trx is omitted from the reaction (data not shown), lending further support to the idea that a specific blockade of DNA unwinding activity results from the strong interaction of the DNA polymerase with gp4 on the lagging strand of the model replication fork. Together our results show the assembly of a functional priming complex on a replication fork mimic that properly orients gp4 for DNA unwinding and engages two copies of gp5/Trx.

Key protein contacts stabilizing the priming complex

The N-terminal ZBD of gp4 functions in the sequence-specific recognition of PRS sites (32) and has a direct role in primer handoff to gp5/Trx during the initiation of Okazaki fragment synthesis (19). However, recent reports have indicated that primer utilization by gp5/Trx can be stimulated by a variant of gp4 that lacks the ZBD (24) and that an RNA-dependent priming complex containing gp5/Trx and gp4 Δ ZBD can be observed by fluorescence anisotropy on ssDNA (25). Our results in figure 1 demonstrate that on a ssDNA substrate the ZBD of gp4 markedly stimulates primer utilization by gp5/Trx. We investigated the importance of the ZBD in priming complex assembly on fork substrates using unwinding assays (Figure 7C). In contrast to wild-type gp4 (Figure 7B), the helicase activity of gp4 Δ ZBD is not blocked by addition of gp5/Trx and a terminated RNA primer, confirming that the ZBD plays a crucial role in stabilizing the interaction of gp4 with gp5/Trx on a fork-shaped DNA.

The gp5 polymerase contains a unique four residue loop (residues 401–404) that lies in the DNA binding crevice at the base of the thumb subdomain (26) where it can support primer utilization during the handoff from gp4 (41). To investigate if this loop is important for the priming complex, we tested the ability of a gp5 Δ 401–404/Trx mutant polymerase lacking the loop to block the helicase activity of wild-type gp4 on a fork-shaped DNA. Using

conditions that promote a stable priming complex of wild-type gp5/Trx and gp4 on a fork-shaped DNA (Figure 7B), the gp5 Δ 401–404 mutant polymerase is unable to block DNA unwinding by gp4 (Figure 7C). These results demonstrate that, like the ZBD of gp4, the 401–404 loop of gp5 plays a critical role in stabilizing priming complex assembly.

Discussion

We have identified conditions for the assembly of an Okazaki fragment initiation complex on DNA in which the hexameric T7 primase-helicase specifically binds two copies of DNA polymerase. The presence of two functional copies of DNA polymerase in this priming complex points to an intimate and predetermined relationship between two core proteins of the T7 replisome, which coordinate leading and lagging synthesis and the initiation of each Okazaki fragment by the priming complex. The gp4 primase-helicase is a central organizer of the T7 replication fork, encircling the lagging strand and providing a physical linkage to leading and lagging strand polymerases. The linkage to the leading strand polymerase is typically thought of as a static interaction between the advancing helicase and the polymerase synthesizing DNA in a continuous manner. Events on the lagging strand are more complicated, as the lagging strand DNA polymerase recycles from a completed Okazaki fragment to the next site of RNA-primed DNA synthesis while keeping pace with the advancing replication fork (42, 43). The stable binding of two DNA polymerase molecules to the primase-helicase protein could reinforce the coupled synthesis of leading and lagging strands of the replication fork and contribute to the processivity of DNA synthesis. In contrast to eukaryotic replisomes that have specialized polymerases for leading and lagging strand synthesis (44), the T7 replisome uses the same enzyme to synthesize both strands. This opens up the possibility that two gp5/Trx molecules bind gp4 in a quasi-equivalent fashion, and that during active replication a single polymerase can interconvert as a leading or a lagging strand polymerase. This concept is further supported by the dynamic structure of the gp4 with its multiple, flexibly tethered primase domains (33) that could service either polymerase molecule to prime lagging strand synthesis.

The involvement of two polymerases in the T7 priming complex compared to the three polymerase replisome of *E. coli* (4) suggests that extra copies of gp5/Trx may be unnecessary for processive replication of the smaller T7 genome (39,937 bp, (45)) compared to the *E. coli* genome (4.6 Mbp; (46)). However, a counterargument can be found in the relatively small T4 genome (168,903 bp, (47)) and evidence for a third polymerase in a subpopulation of T4 replisomes visualized by electron microscopy (48). Whereas the number of polymerases in the *E. coli* replisome is determined by the number of tau subunits in the clamp loader (4), the observation of two gp5/Trx polymerases in the T7 priming complex is likely driven by intimate contacts between the DNA polymerase and the gp4 primase-helicase.

The assembly of two molecules of gp5/Trx in a functional priming complex with gp4 requires two specific protein contacts. The ZBD of gp4 transfers the RNA primer from the RNA polymerase domain of gp4 to the active site of gp5/Trx (19, 23), and our results demonstrate the importance of the ZBD in forming a stable, functional priming complex with gp5/Trx on DNA. Two recent reports (24, 25) have suggested that the ZBD is not required for RNA primer utilization by gp5/Trx. As reported in ref (25), we confirmed that an RNA-dependent priming complex can be formed between gp4 Δ ZBD and gp5/Trx on ssDNA (Supplemental Figure S1). However, the complex lacking the ZBD is not functional in a primer extension assay (Figure 1B) and is unable to stall gp4 helicase activity on an artificial replication fork (Figure 7C). In ref (24), the coupled synthesis of DNA strands in a rolling circle replication reaction is supported by the gp4 Δ ZBD protein at very high concentrations of a synthetic primer. However, for efficient coupled replication activity with

the *de novo* synthesis of primers for lagging strand synthesis, the ZBD of the gp4 primase-helicase protein is essential (24). Additionally, we also find that a unique four residue loop found in gp5/Trx (26, 41) contributes strongly to priming complex formation on a forked DNA. Our results clearly show that the ZBD of gp4 and the 401–404 loop of gp5/Trx are key determinants in T7 priming complex formation.

Similar results are seen for gp4 bound to a model replication fork. The RNA-dependent contact between gp4 and the 5' tail of the forked substrate, corresponding to the lagging strand of a replication fork, also incorporates two molecules of the gp5/Trx polymerase. The second polymerase is capable of binding a primed template DNA (Figure 6), demonstrating that both gp5/Trx molecules in the priming complex are functional. Our results contrast with a recent report that only one gp5/Trx assembles with gp4 in the T7 priming complex (25). We see no evidence of an intermediate with one polymerase bound to the gp4 hexamer on ssDNA or on the forked DNA substrate, even under limiting polymerase concentrations. This suggests that gp4 preferentially binds two copies of gp5/Trx, which could satisfy the requirements for simultaneous replication of the leading and lagging strands of the replication fork. It has been established that the lagging strand polymerase forms an intimate contact with the N-terminal domain of gp4 and the RNA primer (19, 23), but it remains to determine the mode of binding of the second gp5/Trx in the priming complex. A recent report has suggested that binding of the leading strand gp5/Trx by gp4 occurs through two interactions (18). The first occurs at a cleft formed by two monomers of gp4 that bind the palm domain of gp5 while the second is an electrostatic interaction between the C-terminal tail of gp4 binding a basic patch on the polymerase. Whether the second gp5/Trx molecule in the priming complex binds via this electrostatic mode awaits further experimental verification, although it is clear that neither the C-terminal acidic tail of gp4 (Figure 3) nor the Trx processivity factor (Supplementary Figure S2) are required to bind two DNA polymerase molecules in the priming complex.

Our results demonstrate that the RNA-dependent contact between gp5/Trx and gp4 on a model replication fork is sufficient to stall DNA unwinding, and have implications for coordinated replication of both the leading and lagging DNA strands. Lee *et al.* propose that the synthesis and handoff of an RNA primer from gp4 to gp5/Trx causes leading strand synthesis to pause so that replication fork progression is tightly coupled with the synthesis of both strands (49). Replication fork pausing is attributed to an intimate contact between gp4 and the leading strand polymerase. An alternative model proposed by Pandey *et al.* predicts no replisome pausing and the formation of a priming loop that enables gp4 to maintain contact with its oligoribonucleotide product and the PRS even while its associated helicase activity advances the replication fork (50). Both models of coordinated synthesis by the T7 replisome emphasize the functional interactions of gp4 with leading and lagging strand polymerases, which is additionally illustrated by a complete block of the rolling circle replication reaction caused by strand-specific termination of lagging strand synthesis (43). The ability to block the DNA unwinding activity of gp4 by the formation of a stalled priming complex (Figure 7) is further evidence of a very stable interaction between gp4 and gp5/Trx.

The observation that two gp5/Trx molecules associate with the priming complex suggests that gp5/Trx covers multiple subunits of the hexameric gp4 protein, excluding binding by additional polymerases. The mode of interaction between gp4 and gp5/Trx in the priming complex is distinct from the electrostatic interaction seen in the absence of DNA (16) since the C-terminal tail of gp4 is not required in the priming complex. Previous experiments using surface plasmon resonance have suggested that three copies of gp5/Trx can bind a gp4 hexamer in the absence of DNA (51), which brings up the intriguing question of whether the stoichiometry of the T7 replisome changes during different stages of replication. The T7

replisome is dynamic and can exchange with polymerases from bulk solution while continuing DNA synthesis (15, 17) creating the possibility for other compositions of subunits that may assemble at different stages of the replication cycle.

Supplementary Material

Refer to Web version on PubMed Central for supplementary material.

Acknowledgments

We thank Roberto Galletto and Roger Klein for their assistance with analytical ultracentrifugation experiments and members of the Ellenberger group for helpful discussions. This work was supported by the National Institutes of Health (GM055390) and funds from Washington University.

Abbreviations

gp5	gene 5 DNA polymerase
Trx	thioredoxin
gp4	gene 4 primase-helicase
ssDNA	single-stranded DNA
gp2.5	gene 2.5 single stranded DNA binding protein
ZBD	zinc binding domain of gp4
PRS	primase recognition sequence
gp5_SA_TA	gp5 containing a double mutation (D5A, E7A) in the exonuclease domain
gp4E343Q	full-length gp4 containing an E343Q mutation
gp4ΔZBD	gp4 variant that lacks the N-terminal zinc binding domain
gp4CΔ17	gp4 lacking the C-terminal 17 acids
gp4E343QCΔ17	gp4 mutant containing an E343Q mutation and lacking the C-terminal 17 amino acids

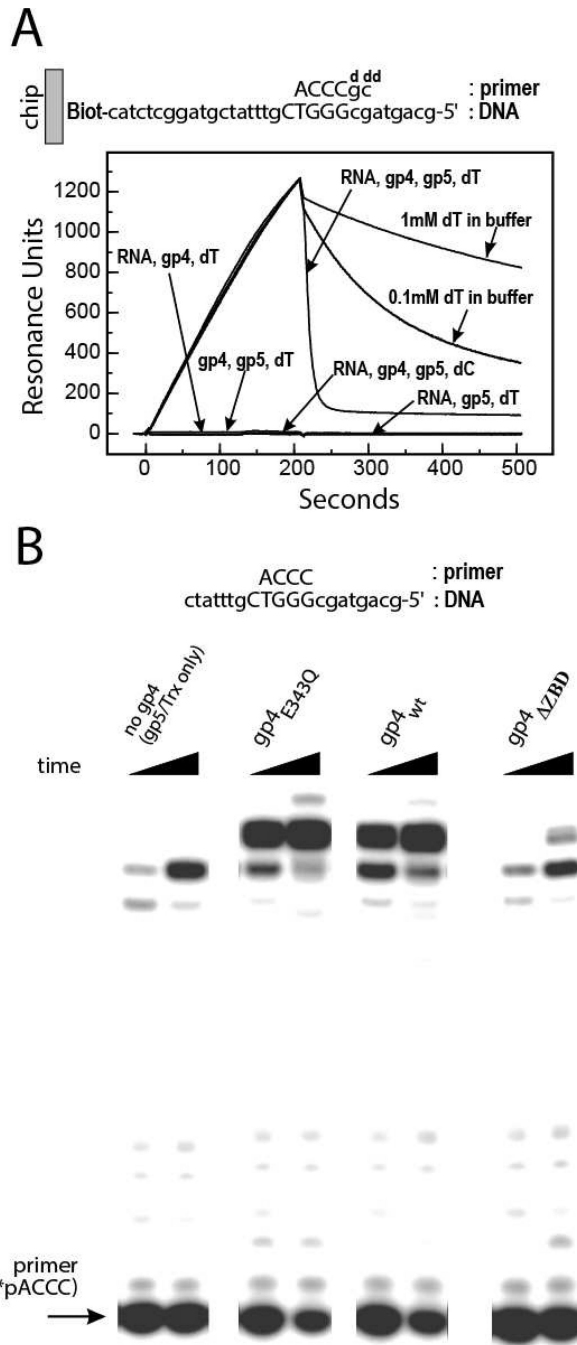
References

1. Langston LD, Indiani C, O'Donnell M. Whither the replisome: emerging perspectives on the dynamic nature of the DNA replication machinery. *Cell Cycle*. 2009; 8:2686–2691. [PubMed: 19652539]
2. McInerney P, Johnson A, Katz F, O'Donnell M. Characterization of a triple DNA polymerase replisome. *Mol. Cell*. 2007; 27:527–538. [PubMed: 17707226]
3. Georgescu RE, Kurth I, O'Donnell ME. Single-molecule studies reveal the function of a third polymerase in the replisome. *Nat. Struct. Mol. Biol.* 2011; 19:113–116. [PubMed: 22157955]
4. Reyes-Lamothe R, Sherratt DJ, Leake MC. Stoichiometry and architecture of active DNA replication machinery in *Escherichia coli*. *Science*. 2010; 328:498–501. [PubMed: 20413500]
5. Lia G, Michel B, Allemand J-F. Polymerase exchange during Okazaki fragment synthesis observed in living cells. *Science*. 2012; 335:328–331. [PubMed: 22194411]
6. Flower AM, McHenry CS. The gamma subunit of DNA polymerase III holoenzyme of *Escherichia coli* is produced by ribosomal frameshifting. *Proc. Natl. Acad. Sci. U.S.A.* 1990; 87:3713–3717. [PubMed: 2187190]

7. Gao D, McHenry CS. Tau binds and organizes Escherichia coli replication proteins through distinct domains. Domain IV, located within the unique C terminus of tau, binds the replication fork, helicase, DnaB. *J. Biol. Chem.* 2001; 276:4441–4446. [PubMed: 11078744]
8. McHenry CS. Purification and characterization of DNA polymerase III'. Identification of tau as a subunit of the DNA polymerase III holoenzyme. *J. Biol. Chem.* 1982; 257:2657–2663. [PubMed: 7037770]
9. Kim S, Dallmann HG, McHenry CS, Marians KJ. Coupling of a replicative polymerase and helicase: a tau-DnaB interaction mediates rapid replication fork movement. *Cell.* 1996; 84:643–650. [PubMed: 8598050]
10. Macneill S. Composition and dynamics of the eukaryotic replisome: a brief overview. *Subcell. Biochem.* 2012; 62:1–17. [PubMed: 22918577]
11. Trakselis MA, Mayer MU, Ishmael FT, Roccasecca RM, Benkovic SJ. Dynamic protein interactions in the bacteriophage T4 replisome. *Trends Biochem. Sci.* 2001; 26:566–572. [PubMed: 11551794]
12. Mueser TC, Hinerman JM, Devos JM, Boyer RA, Williams KJ. Structural analysis of bacteriophage T4 DNA replication: a review in the Virology Journal series on bacteriophage T4 and its relatives. *Virol. J.* 2010; 7:359. [PubMed: 21129204]
13. Hamdan SM, Richardson CC. Motors, switches, and contacts in the replisome. *Annu. Rev. Biochem.* 2009; 78:205–243. [PubMed: 19298182]
14. Lee S-J, Richardson CC. Choreography of bacteriophage T7 DNA replication. *Curr. Opin. Chem. Biol.* 2011; 15:580–586. [PubMed: 21907611]
15. Hamdan SM, Johnson DE, Tanner NA, Lee J-B, Qimron U, Tabor S, van Oijen AM, Richardson CC. Dynamic DNA helicase-DNA polymerase interactions assure processive replication fork movement. *Mol. Cell.* 2007; 27:539–549. [PubMed: 17707227]
16. Zhang H, Lee S-J, Zhu B, Tran NQ, Tabor S, Richardson CC. Helicase-DNA polymerase interaction is critical to initiate leading-strand DNA synthesis. *Proc. Natl. Acad. Sci. U.S.A.* 2011; 108:9372–9377. [PubMed: 21606333]
17. Loparo JJ, Kulczyk AW, Richardson CC, van Oijen AM. Simultaneous single-molecule measurements of phage T7 replisome composition and function reveal the mechanism of polymerase exchange. *Proc. Natl. Acad. Sci. U.S.A.* 2011; 108:3584–3589. [PubMed: 21245349]
18. Kulczyk AW, Akabayov B, Lee S-J, Bostina M, Berkowitz SA, Richardson CC. An Interaction between DNA Polymerase and Helicase is Essential for the High Processivity of the Bacteriophage T7 Replisome. *J. Biol. Chem.* 2012; 287:39050–39060. [PubMed: 22977246]
19. Kato M, Ito T, Wagner G, Ellenberger T. A molecular handoff between bacteriophage T7 DNA primase and T7 DNA polymerase initiates DNA synthesis. *J. Biol. Chem.* 2004; 279:30554–30562. [PubMed: 15133047]
20. Kato M, Frick DN, Lee J, Tabor S, Richardson CC, Ellenberger T. A complex of the bacteriophage T7 primase-helicase and DNA polymerase directs primer utilization. *J. Biol. Chem.* 2001; 276:21809–21820. [PubMed: 11279245]
21. Mendelman LV, Notarnicola SM, Richardson CC. Roles of bacteriophage T7 gene 4 proteins in providing primase and helicase functions in vivo. *Proc. Natl. Acad. Sci. U.S.A.* 1992; 89:10638–10642. [PubMed: 1438259]
22. Lee S-J, Zhu B, Akabayov B, Richardson CC. Zinc-binding domain of the bacteriophage T7 DNA primase modulates binding to the DNA template. *J. Biol. Chem.* 2012; 287:39030–39040. [PubMed: 23024359]
23. Kato M, Ito T, Wagner G, Richardson CC, Ellenberger T. Modular architecture of the bacteriophage T7 primase couples RNA primer synthesis to DNA synthesis. *Mol. Cell.* 2003; 11:1349–1360. [PubMed: 12769857]
24. Zhu B, Lee S-J, Richardson CC. Direct role for the RNA polymerase domain of T7 primase in primer delivery. *Proc. Natl. Acad. Sci. U.S.A.* 2010; 107:9099–9104. [PubMed: 20439755]
25. Kulczyk AW, Richardson CC. Molecular interactions in the priming complex of bacteriophage T7. *Proc. Natl. Acad. Sci. U.S.A.* 2012; 109:9408–9413. [PubMed: 22645372]
26. Doublie S, Tabor S, Long AM, Richardson CC, Ellenberger T. Crystal structure of a bacteriophage T7 DNA replication complex at 2.2 Å resolution. *Nature.* 1998; 391:251–258. [PubMed: 9440688]

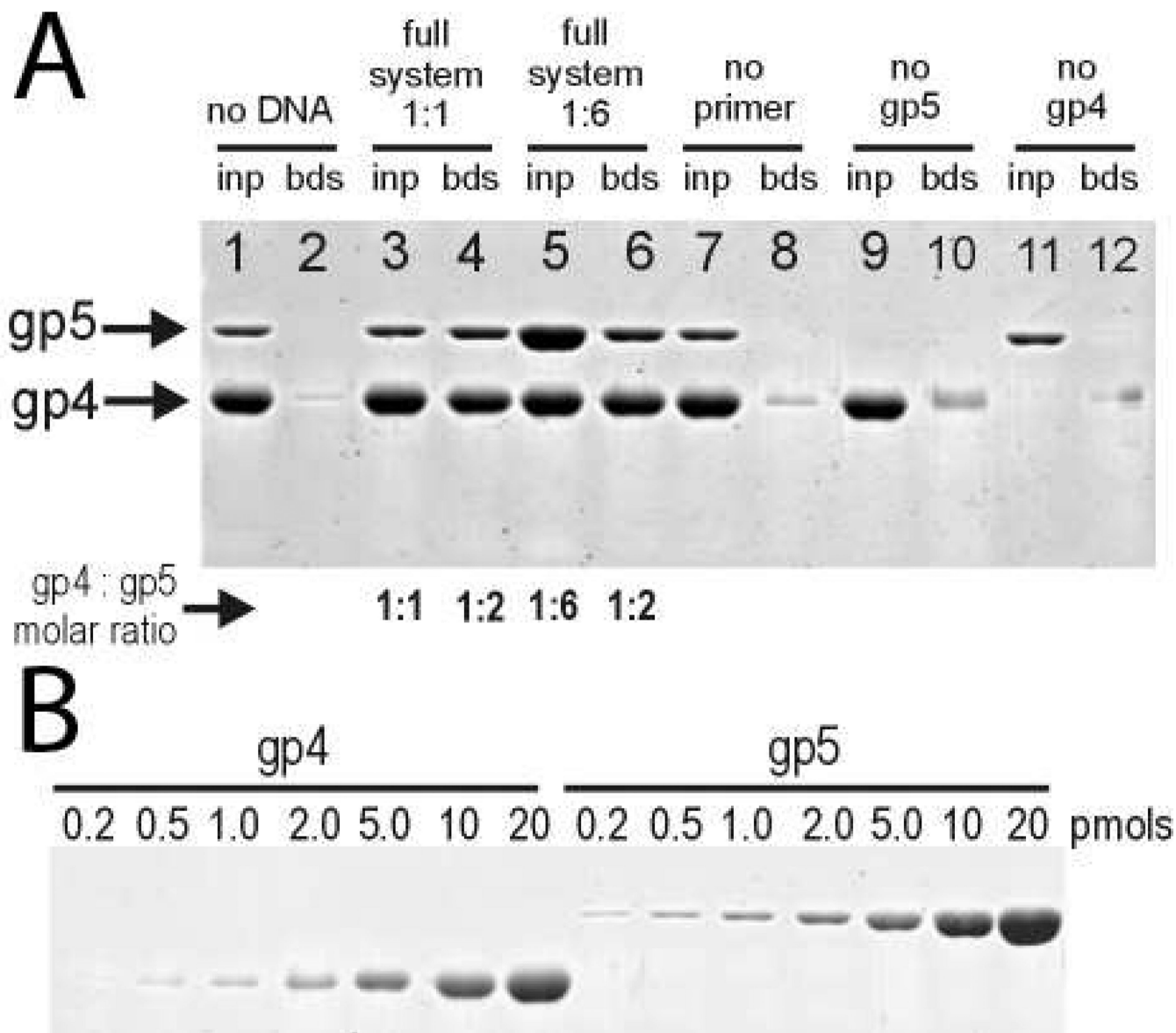
27. Picha KM, Patel SS. Bacteriophage T7 DNA helicase binds dTTP, forms hexamers, and binds DNA in the absence of Mg²⁺. The presence of dTTP is sufficient for hexamer formation and DNA binding. *J. Biol. Chem.* 1998; 273:27315–27319. [PubMed: 9765257]
28. Lee SJ, Richardson CC. Essential lysine residues in the RNA polymerase domain of the gene 4 primase-helicase of bacteriophage T7. *J. Biol. Chem.* 2001; 276:49419–49426. [PubMed: 11673465]
29. Patel SS, Wong I, Johnson KA. Pre-steady-state kinetic analysis of processive DNA replication including complete characterization of an exonuclease-deficient mutant. *Biochemistry*. 1991; 30:511–525. [PubMed: 1846298]
30. Schuck P. Size-distribution analysis of macromolecules by sedimentation velocity ultracentrifugation and lamm equation modeling. *Biophys. J.* 2000; 78:1606–1619. [PubMed: 10692345]
31. Balbo A, Brown PH, Braswell EH, Schuck P. Measuring protein-protein interactions by equilibrium sedimentation. *Curr. Protoc. Immunol.* 2007 *Chapter 18*, Unit 18.8.
32. Kusakabe T, Hine AV, Hyberts SG, Richardson CC. The Cys4 zinc finger of bacteriophage T7 primase in sequence-specific single-stranded DNA recognition. *Proc. Natl. Acad. Sci. U.S.A.* 1999; 96:4295–4300. [PubMed: 10200256]
33. Toth EA, Li Y, Sawaya MR, Cheng Y, Ellenberger T. The crystal structure of the bifunctional primase-helicase of bacteriophage T7. *Mol. Cell.* 2003; 12:1113–1123. [PubMed: 14636571]
34. Crampton DJ, Ohi M, Qimron U, Walz T, Richardson CC. Oligomeric states of bacteriophage T7 gene 4 primase/helicase. *J. Mol. Biol.* 2006; 360:667–677. [PubMed: 16777142]
35. Crampton DJ, Mukherjee S, Richardson CC. DNA-induced switch from independent to sequential dTTP hydrolysis in the bacteriophage T7 DNA helicase. *Mol. Cell.* 2006; 21:165–174. [PubMed: 16427007]
36. Kim D-E, Narayan M, Patel SS. T7 DNA helicase: a molecular motor that processively and unidirectionally translocates along single-stranded DNA. *J. Mol. Biol.* 2002; 321:807–819. [PubMed: 12206763]
37. Satapathy AK, Crampton DJ, Beauchamp BB, Richardson CC. Promiscuous usage of nucleotides by the DNA helicase of bacteriophage T7: determinants of nucleotide specificity. *J. Biol. Chem.* 2009; 284:14286–14295. [PubMed: 19297330]
38. Picha KM, Ahnert P, Patel SS. DNA binding in the central channel of bacteriophage T7 helicase-primase is a multistep process. Nucleotide hydrolysis is not required. *Biochemistry*. 2000; 39:6401–6409. [PubMed: 10828954]
39. Patel SS, Pandey M, Nandakumar D. Dynamic coupling between the motors of DNA replication: hexameric helicase, DNA polymerase, and primase. *Curr. Opin. Chem. Biol.* 2011; 15:595–605. [PubMed: 21865075]
40. Doublié S, Ellenberger T. The mechanism of action of T7 DNA polymerase. *Curr. Opin. Struct. Biol.* 1998; 8:704–712. [PubMed: 9914251]
41. Chowdhury K, Tabor S, Richardson CC. A unique loop in the DNA-binding crevice of bacteriophage T7 DNA polymerase influences primer utilization. *Proc. Natl. Acad. Sci. U.S.A.* 2000; 97:12469–12474. [PubMed: 11050188]
42. Debyser Z, Tabor S, Richardson CC. Coordination of leading and lagging strand DNA synthesis at the replication fork of bacteriophage T7. *Cell.* 1994; 77:157–166. [PubMed: 8156591]
43. Lee J, Chastain PD, Kusakabe T, Griffith JD, Richardson CC. Coordinated leading and lagging strand DNA synthesis on a minicircular template. *Mol. Cell.* 1998; 1:1001–1010. [PubMed: 9651583]
44. Nick McElhinny SA, Gordenin DA, Stith CM, Burgers PMJ, Kunkel TA. Division of labor at the eukaryotic replication fork. *Mol. Cell.* 2008; 30:137–144. [PubMed: 18439893]
45. Dunn JJ, Studier FW. Complete nucleotide sequence of bacteriophage T7 DNA and the locations of T7 genetic elements. *J. Mol. Biol.* 1983; 166:477–535. [PubMed: 6864790]
46. Blattner FR, Plunkett G, Bloch CA, Perna NT, Burland V, Riley M, Collado-Vides J, Glasner JD, Rode CK, Mayhew GF, Gregor J, Davis NW, Kirkpatrick HA, Goeden MA, Rose DJ, Mau B, Shao Y. The complete genome sequence of Escherichia coli K-12. *Science*. 1997; 277:1453–1462. [PubMed: 9278503]

47. Miller ES, Kutter E, Mosig G, Arisaka F, Kunisawa T, Rüger W. Bacteriophage T4 genome. *Microbiol. Mol. Biol. Rev.* 2003; 67:86–156. [PubMed: 12626685]
48. Nossal NG, Makhov AM, Chastain PD, Jones CE, Griffith JD. Architecture of the bacteriophage T4 replication complex revealed with nanoscale biopointers. *J. Biol. Chem.* 2007; 282:1098–1108. [PubMed: 17105722]
49. Lee J-B, Hite RK, Hamdan SM, Xie XS, Richardson CC, van Oijen AM. DNA primase acts as a molecular brake in DNA replication. *Nature.* 2006; 439:621–624. [PubMed: 16452983]
50. Pandey M, Syed S, Donmez I, Patel G, Ha T, Patel SS. Coordinating DNA replication by means of priming loop and differential synthesis rate. *Nature.* 2009; 462:940–943. [PubMed: 19924126]
51. Guo S, Tabor S, Richardson CC. The linker region between the helicase and primase domains of the bacteriophage T7 gene 4 protein is critical for hexamer formation. *J. Biol. Chem.* 1999; 274:30303–30309. [PubMed: 10514525]

**Figure 1.**

A) Surface plasmon resonance analysis of the T7 priming complex. A stable protein complex is formed on an immobilized ssDNA containing a primase recognition site (PRS) when both gp4 and gp5/Trx are present with a 2',3'-dideoxy terminated RNA primer and dTTP matching the template sequence. Increasing the concentration of dTTP in the reaction buffer slows the dissociation of proteins from the DNA. B) Gp4 stimulates primer utilization by gp5/Trx. The gp4 primase-helicase is required for efficient extension of a synthetic RNA primer by the gp5/Trx polymerase. The ZBD of gp4 strongly contributes to the initiation of DNA synthesis from an RNA primer (compare wt and Δ ZBD reactions). The helicase activity of gp4 is not required for primer utilization by gp5/Trx (compare wt and E343Q

reactions). The primer extension products include the fully extended RNA-DNA product as well as n-1 and n-2 products, as observed previously (23). Minor radioactive species migrating above the labeled RNA primer are invariant during the course of the primer extension reaction and likely correspond to impurities from RNA synthesis that could not be extended by the DNA polymerase.

**Figure 2.**

Quantitative analysis of proteins pulled down with a biotinylated ssDNA containing a PRS. A) A priming complex is purified on ssDNA when gp4, gp5/Trx, a terminated primer, and DNA are all present. The same ratio of gp5/Trx to gp4 hexamer is purified in the presence of both limiting and saturating concentrations of DNA polymerase (compare lanes 4 and 6). A small amount of streptavidin is observed leaching from the beads (lane 12). The streptavidin is similar in size to gp4 but does not affect the calculated stoichiometry. Analysis of the protein staining intensities using the calibration gel shown in B) reveals that two copies of gp5/Trx purify with a gp4 hexamer.

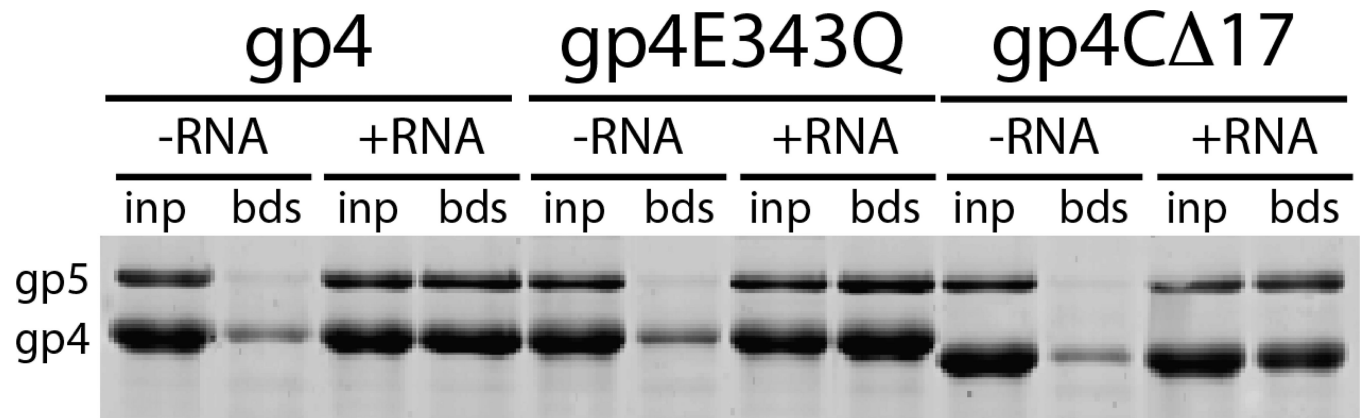
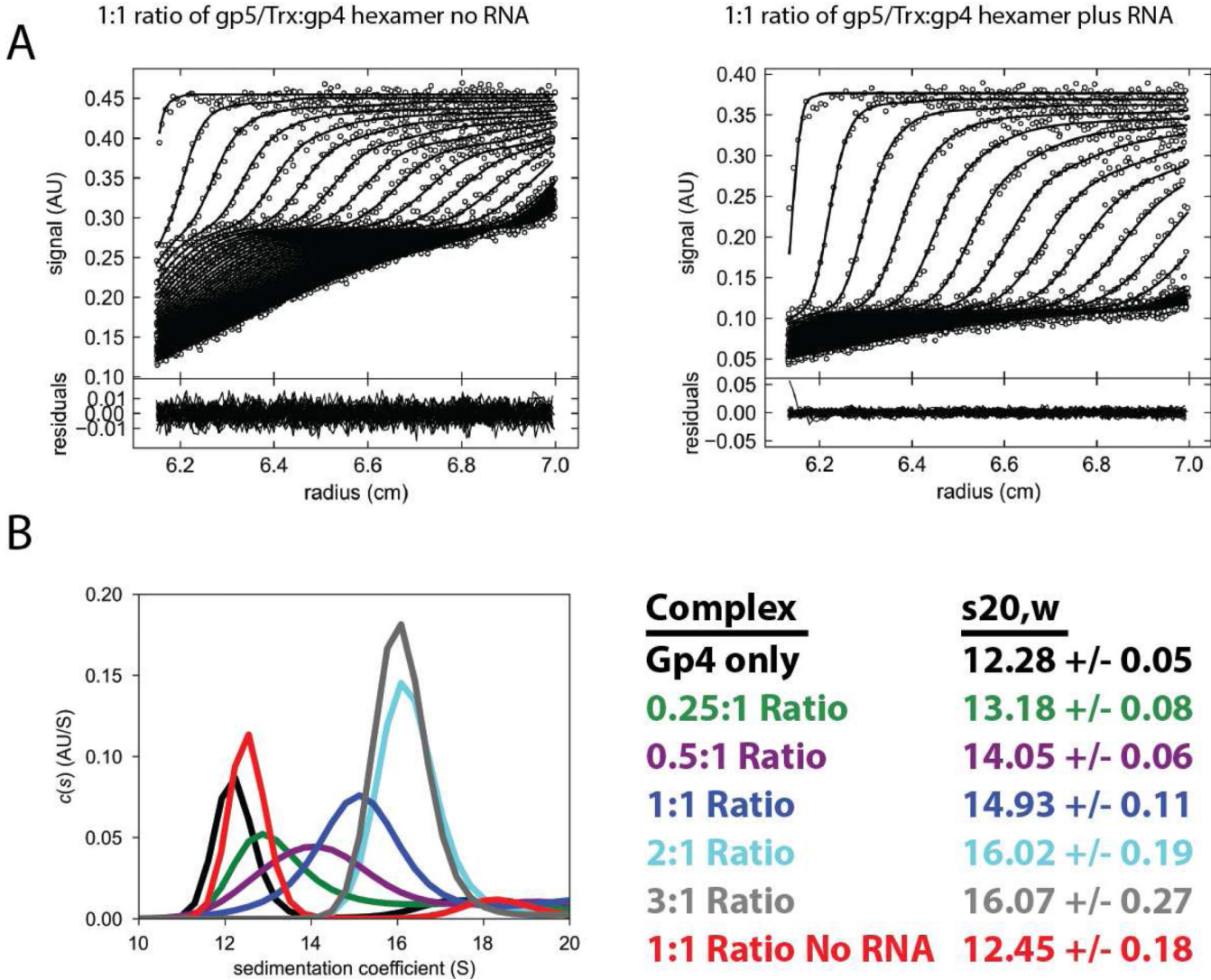
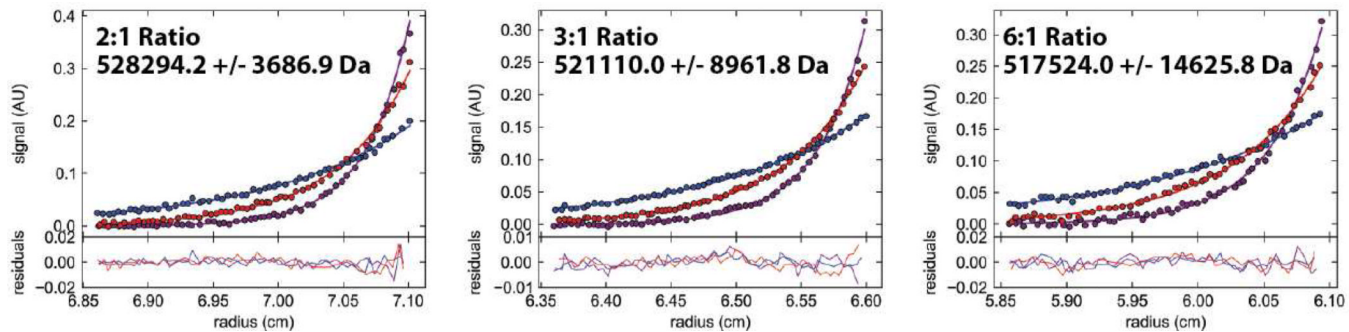


Figure 3.

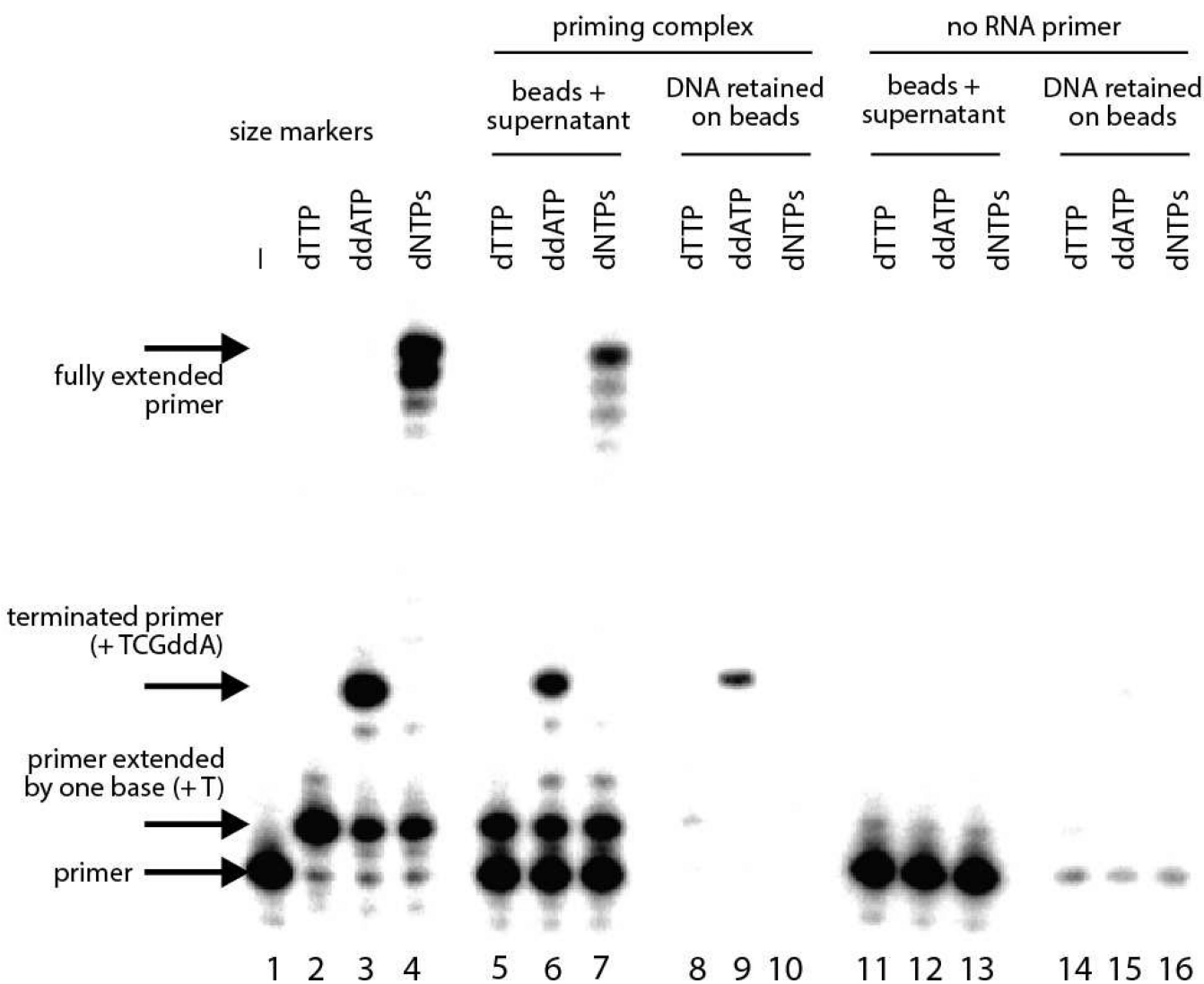
A mutation of the catalytic base in the helicase domain of gp4 (gp4E343Q) that abolishes gp4 DNA translocation activity (35) does not alter the subunit composition of the priming complex formed in the presence of dTTP (compare gp4 to gp4E343Q). Additionally, the C-terminal tail of gp4 can be deleted (gp4C Δ 17) without affecting the association of two copies of gp5/Trx in the priming complex.

**Figure 4.**

Velocity sedimentation reveals a 2:1 ratio of T7 DNA polymerase and hexameric primase-helicase in the priming complex. (A) Analytical sedimentation velocity profiles for an input 1:1 ratio of gp5/Trx:gp4 hexamer demonstrate that the addition of a terminated primer results in a larger complex formed on the labeled ssDNA, shifting the sedimentation coefficient from 12.5 S to 14.9 S. (B) Sedimentation velocity analysis of the priming complex. A titration of gp5/Trx against a fixed concentration (3 μ M) of gp4 shows a shift in the sedimentation coefficient that saturates at a 2:1 molar ratio of gp5/Trx:gp4 hexamer. Omission of the terminated RNA primer results in a smaller complex, demonstrating that the larger complex observed upon titration with polymerase is the priming complex.

**Figure 5.**

The buoyant mass of the priming complex indicates two copies of gp5/Trx are bound to a gp4 hexamer. Gp4 was mixed with ssDNA, a terminated RNA primer, dTTP, and different concentrations of gp5/Trx, and the resulting complexes were analyzed by sedimentation equilibrium at 5,000 (blue), 7,000 (red) and 9,000 (purple) RPM. At all input ratios of gp5/Trx:gp4 hexamer the complexes sediment with a mass consistent with two polymerase molecules binding a gp4 hexamer in the priming complex.

**Figure 6.**

The second copy of DNA polymerase in the T7 priming complex is competent for DNA synthesis. The priming complex was isolated on a biotinylated ssDNA containing a PRS using a terminated RNA primer and dTTP. After purification, a radiolabeled primer-template DNA was added to the complex along with dNTPs and ddATP to terminate the primer-template, and the complex was again isolated in the presence of high concentrations of dTTP and dGTP stabilize the DNA polymerases on the biotinylated ssDNA and radiolabeled primer-template DNA, respectively. The radiolabeled primer-template DNA can be co-purified with the priming complex only when terminated by a dideoxy nucleotide (compare lanes 8–10). The primer-template fails to purify if the RNA primer is omitted (lane 15), demonstrating that the primer-template is associated with the priming complex.

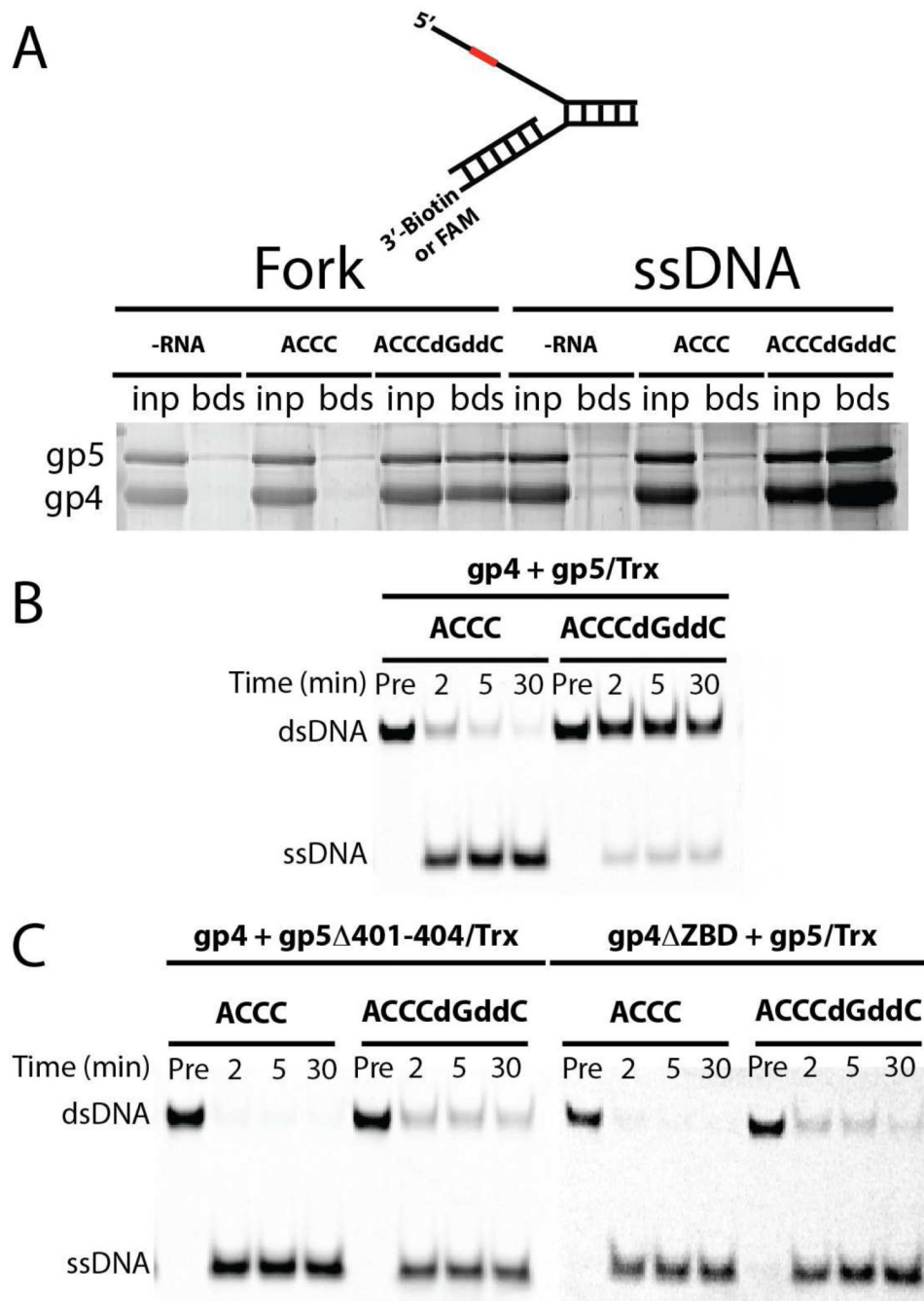


Figure 7.
Assembly of a stable priming complex stalls the unwinding of a fork-shaped DNA. (A) Cartoon representation of fork-shaped substrates used in these experiments. The PRS where the priming complex assembles is shown in red. A priming complex can be purified on both a fork-shaped substrate as well as ssDNA, and both substrates require a terminated RNA primer. The similar protein staining profiles for both complexes confirm they contain two gp5/Trx molecules in complex with gp4. (B) The ability of gp4 to unwind a fork-shaped DNA was tested in the presence of both a terminated and non-terminated RNA primer. Gp4 can efficiently unwind a fork in the presence of gp5/Trx and a non-terminated RNA primer. However, a terminated RNA primer inhibits unwinding activity, demonstrating the

formation of a stable priming complex. (C) A DNA polymerase variant with a deletion of residues 401–404 shows this loop is required to stall the DNA unwinding activity of gp4 in the priming complex. Additionally, the N-terminal ZBD of gp4 is critical for the interaction with gp5/Trx.

Table I

Oligonucleotides used in this study. For DNA oligonucleotides, primase recognition sequences are shown in capital letters.

RNA/DNA substrate	Figure used
ACCC (RNA)	Figures 1B and 7
ACCCdGddC (RNA)	Figures 1A, 2, 3, 4, 5, 6, 7, S1, S2
5'-gcagtagcGGGTcgtttatcgtaggctctac-3'-TEG-Biotin	Figures 1A, 7A
5'-gcagtagcGGGTcgtttat-3'-TEG-Biotin	Figures 2,3, 6, S1, S2
5'-gcagtagcGGGTcgtttac-3'	Figure 1B
5'-gcagtagcGGGTcgtttac-3'-FAM	Figures 4 and 5
5'-cgagccgactcgagcatccgctacgtacg-3'	Figure 6
5'-cgtacgtaaggatgc-3'	Figure 6
5'-gcagtagcGGGTcgtttatcgtaggctctacggaggcgagcgtgcttagcc-3'	Figure 7
5'-ggctaaggcacgtcgccctctgtcacccagtgactggactggccgtggtttcg-3'-TEG-Biotin	Figure 7A
5'-cgaaaaccacggccagtgcc-3'	Figure 7A
5'-ggctaaggcacgtcgcccttttttttttttttt-3'-FAM	Figure 7B and 7C
5'-aaaaaaaaaaaaaaaaaaaa	Figure 7B and 7C